Paper ID ICLASS06-095
EFFECTS OF FLUID PROPERTIES ON THE BUBBLE INK-JET

Jy-Cheng Chang[1], Jiu-Zhang Lu[2], Wei-Chun Wang[3], Cheng-Hwa Chen[4] and Deng-Guei Yu[5]

[1] Associate Professor, Department of Mechanical Engineering, changjc@ccit.edu.tw
[2] Postgraduate (Ph.D.), School of Defense Science, g970404@ccit.edu.tw
[3] M.Sc., School of Weapon System Engineering, liononar@yahoo.com.tw
[4] M.Sc., School of Weapon System Engineering, alpha0814@yahoo.com.tw
[5]Postgraduate (M.Sc.), School of Weapon System Engineering, g951711@ccit.edu.tw
Chung Cheng Institute of Technology,
National Defense University,
Tashi, Taoyuan 33509, Taiwan, R.O.C.

ABSTRACT The bubble (or thermal) ink-jet printing can be used in the process of the manufacturing P-OLED and one of the critical technologies is the precise drop placement of injection. To study the effects of the fluid properties such as viscosity and surface tension on the injecting and assess the feasibility of the manufacturing P-OLED by using the bubble ink-jet printing, the drop placement accuracy of injection was estimated by alternatively using the spray angle which was derived from the measurements of vertical and horizontal velocities of the droplet. The Particle Dynamic Analyzer (PDA) was used to systematically measure the droplet velocity and size for four fluids in this work. The macro-photography was also used to visualize the detachment process of the liquid jet at the exit of the injector. The typical results are as follow:
1. The estimation of the drop placement accuracy of injection by deriving from the measured velocity and droplet size is practicable.
2. In this experiment, there are some critical fluid properties resulting in lounger breakup length. These results can be adapted to improve the accuracy of jet targeting.
3. The manufacturing P-OLED by using the bubble ink-jet printing is feasible.

Keywords: Bubble Ink-jet Printing, Particle Dynamic Analyzer, Viscosity, Drop Placement

1. INTRODUCTION

It is known that the ink-jet is a non-contact dot-matrix printing technology in which drops of ink are injected from an orifice directly to a specified position on a substrate. Due to its characters of materials efficient, low cost, quiet, high speed, non-contact and computer controllable, the ink-jet technology has been widely used not only in the traditional ink-jet printer but also in many fields such as fueling in the gasoline engine [1], rapid prototyping [2], manufacturing color filters [3-4], polymer micro-lenses, solder bump [5] and polymer organic light emitting diodes (P-OLED) [6] in recent years. Le [7] provided a brief review of the various paths undertaken in the development of ink-jet printing and summarized that in newly emerging markets and applications, significant improvements in print head design and ink formulation are needed to fulfill the high expectations for printer reliability and image durability required for these new applications. Bale et al. [6] described the developments that have been carried out at Cambridge Display Technology to assist in achieving ink-jet printing technology for P-OLED displays. They claimed that there are significant differences between the application of ink-jet printing for graphic arts and P-OLED displays. For printing P-OLED displays it is necessary to achieve a high specification of both the drop placement and drop volume. Therefore, the key requirements for the print head system are that specified targets are met for drop position, drop volume, print reliability and throughput. As Le [7] reported, most of the drop-on demand ink-jet printers of nowadays are using either the thermal or piezoelectric principle. It is also known that the thermal ink-jet method was not the first ink-jet method implemented in a product, but it is the most successful method on the market today. The objective of this study is to investigate the effects of the fluid properties such as viscosity and surface tension on the injecting and assess the feasibility of the manufacturing P-OLED by using the bubble ink-jet printing.

2. EXPERIMENTAL APPARATUS

The macro-photography was used to visualize the detachment process of the liquid jet at the exit of the injector and the Particle Dynamic Analyzer (PDA) was used to systematically measure the droplet velocity and size for different fluids in this work.

2.1 Photography

The macroscopic-lens and high speed CCD camera assembled with a PC and a stroboscope were placed in the appropriate position to observe and record the process of ink-jetting. A 3-D translating stage was used to move the droplet stream to a suitable position for photograph. The thermal ink-jet print head and control system was purposed built and the current pulse with required voltage setting and duration was supplied through the heater. Whenever the heater was ignited the print head started injecting down ward vertically.

2.2 Phase-Doppler System

The two dimensional Particle Dynamic Analyzer (PDA) (or called Phase-Doppler anemometry) allows the

simultaneous measurement of the velocity and size of individual spherical drops injecting from the print head. The measuring position was underneath the print head with 500 μm distance and set on the point where the drop stream will go through. The system is shown schematically in Fig. 1. More details about the PDA system and optical setting were discussed in our previous works [8-9]. The experimental system was assembled with the power supplier (1), the electrical circuit (2) for the print head (3), the stand and 3-way stage (4) for the print head, the laser emitting head (5), the laser receiver head (6), the photo-multiplier and signal processor (7), the laser transmitter (8), the interface and PC (9), the laser (10) and the oscilloscope (11). The macroscopic-lens and high speed CCD camera (12) assembled with a video recorder (13) or PC are also shown in the figure. More details about the photographic system were described in our previous works [10-11]. Figure 2 shows the typical photographs of the ink-jet emitting from a commercial thermal ink-jet print head. It is worth mentioning that there are always satellites following the main drop and the number of satellite can vary from one to seven at the same injecting condition. These photos can assist us in the optical focusing and setting; and evaluating the data of the PDA output in the measurement of the velocity and size of the drop. More details about the satellite will be discussed in the result.

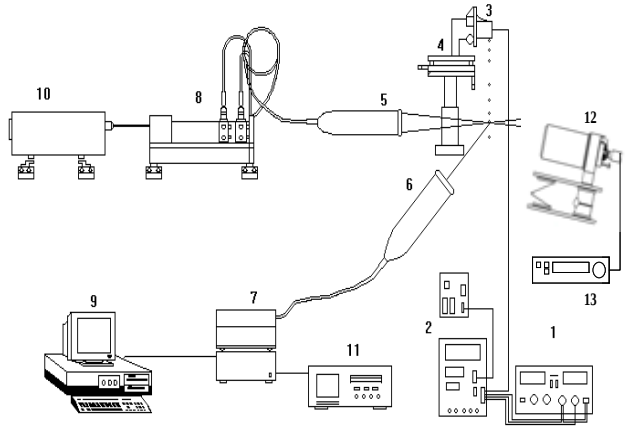

1. power supplier 2. electrical circuit 3. print head
4. stand and 3-way stage 5. laser emitting head
6. laser receiver head
7. photo-multiplier and signal processor
8. laser transmitter 9. interface and PC
10. laser 11. oscilloscope
12. macroscopic-lens and high speed CCD camera
13. video recorder or PC

Fig.1 Schematic of the experimental apparatus.

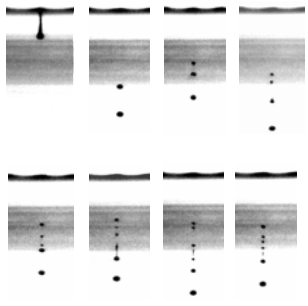

Fig. 2. The typical photographs of the ink-jet emitting from a commercial thermal ink-jet print head.

2.3 Parameter Setting and Fluid Properties

The voltage and duration of pulse current through the heater in thermal ink-jet print head were 14.6 V and 2.6 μs, respectively. The frequency of pulse current resulting in ink injection was set in 1.0 kHz. The location of collection optics from forward scatter in the PDA system is 73 degree where the effect of refractive index changing on the PDA measurement is not sensitive; more details described in our previous work [9]. The tolerance of un-spheroid was set at 30%. To be consistent, all measurements were kept in the same nozzle in the print head in this experiment. An ensemble of at least 40% data was collected for each measurement. The statistical uncertainty in estimating the mean velocity from randomly sampled data was estimated to be below 2%, according to Yanta [12]. As far as the size measurements are concerned, according to Tate [13] the maximum deviation from the actual cumulative distribution is expected to be below 2.5%.

To identify the effects of the fluid properties such as viscosity and surface tension on the injecting, five fluids which are water, water-sugar solutions, water-glycerin solution and PF solution were used in this study (only four fluids were used in the PDA measurement). Table 1 shows their physical properties.

Table 1. Properties of the working fluids at 20˚C.

	$\rho(kg/m^3)$	$\mu(cP)$ or (mN/m^2)	$\sigma(mN/m)$
Water	1,000	0.99	72.4
Water-sugar solution (25%wt)	1,100	2.28	69.0
Water-sugar solution (33.3%wt)	1,150	3.80	71.6
Water-glycerin solution (40%wt)	1,100	3.64	58.9
PF solution (Anisole + TMB)0.7%wt	1,007	4.64	25.35

The viscosity and surface tension were measured by using the Brookfield Dial Viscometer and the CBVP-A3 Surface Tensiometer, respectively.

3. RESULTS

The experimental program was divided into two parts. First, the detachment process for different fluids was investigated by using photography. The second part of the program involved measurements of droplet mean axial and radial velocities and size by phase Doppler anemometry, and then the drop placement accuracy of injection was estimated.

3.1 Detachment Process of the Liquid Jet

Figure 3 shows the photos of the water jet emitting from the print head nozzle in different time since start of injection and as these photos show, the water flows out of the print head in the form of a jet which is similar with the

result of Parrado and González's work [14]; this jet becomes longer as time progresses and its tip gradually becomes more spherical in shape and then the main drop detaches itself from the jet.

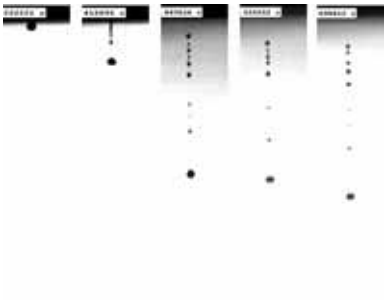

Fig.3 The water jet emitting from the print head nozzle.

It is worth mentioning again that there are always satellites following the main drop and the number of satellite in the water case can vary from 4 to 9 the same injecting condition. To identify the variation of the number of the satellite, about 100 photos which were randomly taken were investigated and the percentage of different number of satellite was estimated. Figure 4 shows the percentage of different number of satellite for water case and indicates that the largest percentage is about 35% for the photo with 7 satellites.

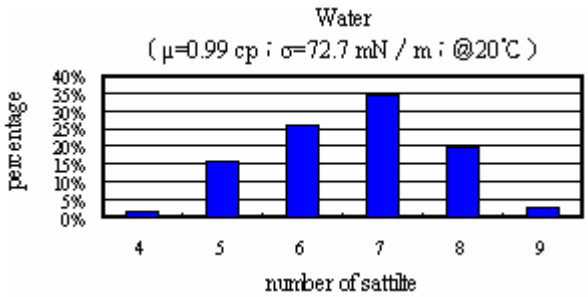

Fig.4 The percentage of different number of satellite for water jet at the same injecting setting.

Figures 5-7 show the photos of the water-sugar solution (25%wt), the water-sugar solution (33.3%wt), water-glycerin solution (40%wt) jets, respectively, and figures 8-10 show the percentages of different number of satellite for these three cases.

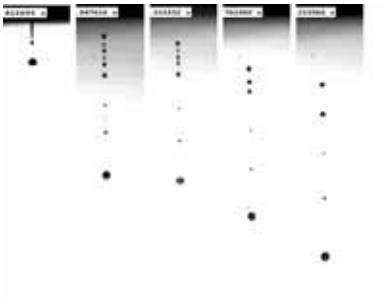

Fig.5 Water-sugar solution (25%wt) drop printing.

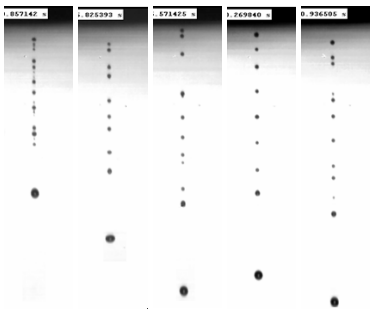

Fig.6 Water-sugar solution (33.3%wt) drop printing.

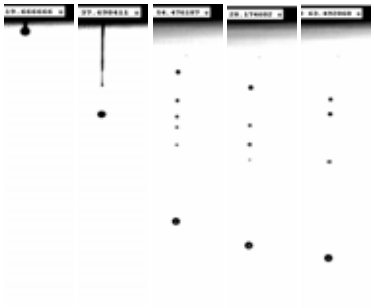

Fig.7 Water-glycerin solution (40%wt) drop printing.

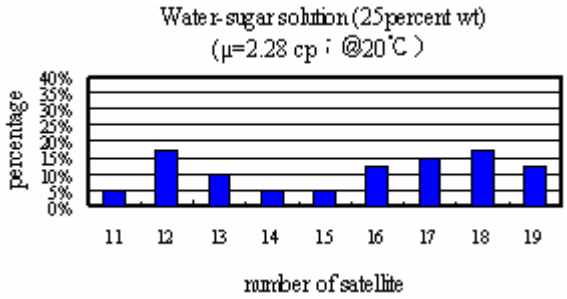

Fig.8 The percentage of different number of satellite for Water-sugar solution (25%wt) jet at the same injecting setting.

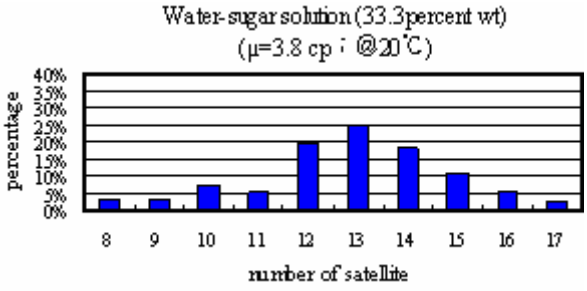

Fig.9 The percentage of different number of satellite for water-sugar solution (33.3%wt) jet at the same injecting setting.

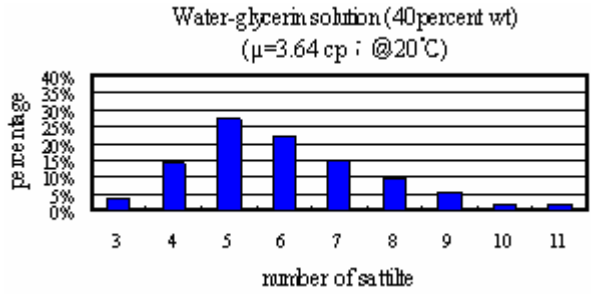

Fig.10 The percentage of different number of satellite for water-glycerin solution (40%wt) jet at the same injecting setting.

Figure 11 shows the jet photos of different fluid with maximum and minimum number of satellite.

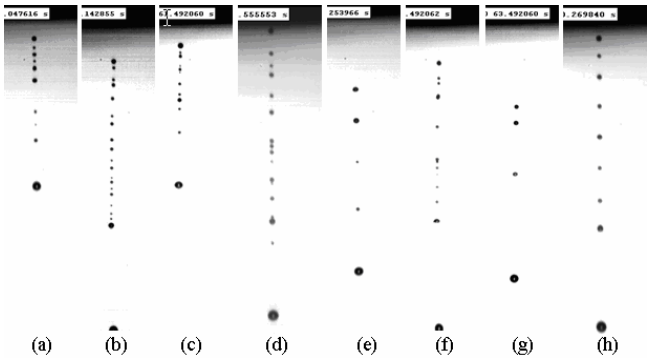

Fig.11 The maximum and minimum numbers of satellite of water, water-sugar solution (25%wt), water-glycerin solution (40%wt) and water-sugar solution (33.3%wt), respectively. (a-d: maximum, e-h: minimum).

Figure 12 shows the minimum to maximum number of satellite against the different fluid.

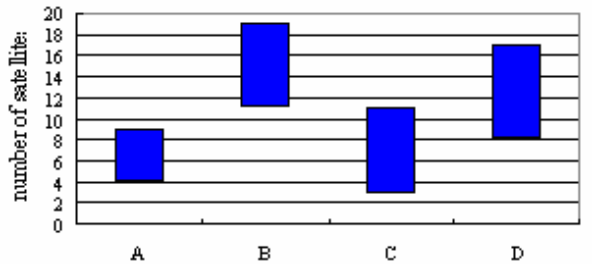

Fig.12 The minimum to maximum number of satellite of water (A), water-sugar solution (25%wt) (B), water-glycerin solution (40%wt) (C) and water-sugar solution (33.3 % wt) (D), respectively.

Closer examination in the photos of the detachment process of the liquid jet, we find that the longer liquid column following the main drop is the more number of satellites in the injection. Also the longer liquid column is the more number of satellites in the injection. It is interesting to note that the breakup length is not linearly proportional to the viscosity.

3.2 Drop Placement Accuracy

According to the results of our previous [15] and this works mentioned above, whenever the liquid emits into the ambiance it always shapes into a column and then the column becomes longer as time progresses; and its tip gradually becomes more spherical in shape and then the main drop detaches itself from the column which integrates into some satellites. For the application of ink-jet printing, all the drops including the main and satellite are expected to be placed at the target. However, the instability of the integration of the liquid column will affect the placement accuracy. Based on our experience, the instability will result in a variation of drop velocity, size and number of satellite. The variation of the radial velocity is much expected to affect the placement accuracy, and the size is expected as well. Therefore, the axial and radial velocities and size of the main drop and satellite were measured by using PDA and the injection angle relative to the axis of the nozzle hole was derived. The spray angle was statistically estimated by using the standard deviation of the injection angle. Finally, involving the drop size the area and accuracy of the drop placement were evaluated.

The injection angle, spray angle and area of drop placement are described below:

3.3 Injection Angle and Spray Angle

Due to the gravity, after leaving the nozzle the jet and drops will move along the axis of the nozzle hole. However, the direction of moving is varied due to the instability of injection and this fact results in scattering of the drop placement. It is almost not practicable to directly derive the placement accuracy by statistically counting dropping places one by one. In this work, the placement is estimated by using the spray angle (called θ) which is derived from the injection angle. Based on the assumption that the drop moves along a straight line, the injection angle is defined as the contained angle between the axis of the nozzle hole and the path of the moving drop. Figure 13 shows the schematic of the injection angle and the spray angle, where the injection angle (α or β) is derived from $\tan^{-1}(V/U)$.

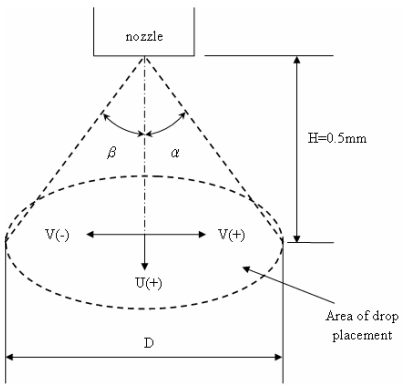

Fig. 13 Injection angle, spray angle and measurement volume.

V and U are the radial and axial component of the drop velocity, respectively, and outputs from the PDA measurement. The injection angle is called α when the radial component is positive and β for negative. As

mentioned before, the measuring position was underneath the print head with 500 μm distance and on the point where the drop stream will go through. It should be mentioned that the effective length of the measuring volume is about 186 μm in this PDA system. The maximum spray angle (θ_{max}) of 4096 samples, which is proportional to the area of the drop placement, is the sum of α_{max} and $|\beta_{min}|$. The mean of the injection angles in 4096 measured data is called the mean spray angle (θ_{mean}) and this angle indicates how consistent the direction of injection is with the ideal axis of nozzle hole. Moreover, the standard deviation (σ) of the injection angle in 4096 measured data indicates how serious the variation of the injection angle is. To avoid biasing the meaning of the injection variation for few extremes of data, the spray angle is defined as six times of the standard deviation of the injection angle (6σ of injection angle) which includes 99.73% of injection angle in 4096 measured data.

3.4 Area of Drop Placement

Based on the assumption of circular placement area, the diameter of the area can be derived from the equation as follow:

$$D=d_{mean}+2H\tan(3\sigma), \quad (1)$$

Where d_{mean} is the mean drop diameter, H is the distance between the exit of the nozzle and the measuring point and σ is the standard deviation of the injection angle.

3.5 Output of PDA and Accuracy of Drop Placement

Figure 14 is the output of PDA measurement which shows the axial velocity (U, m/s), radial velocity (V, m/s) and diameter (μm) of the drop.

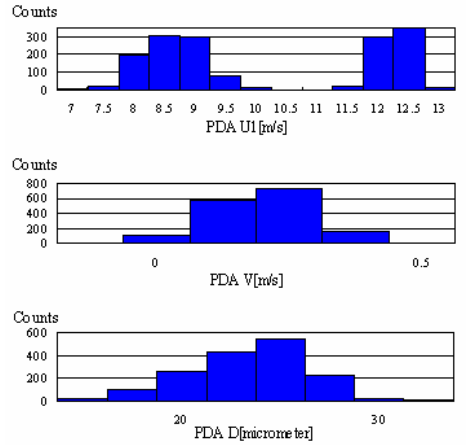

Fig. 14 The output of PDA measurement.

Figure 15 shows the injection angle derived from the above data. On the upper left hand side, the figure shows the velocities (U, V) of 4096 data; and on the upper right hand side, the figure shows the dimensionless of velocities (U/I, V/I), where $I=(U^2+V^2)^{1/2}$ is the length of the velocity vector.

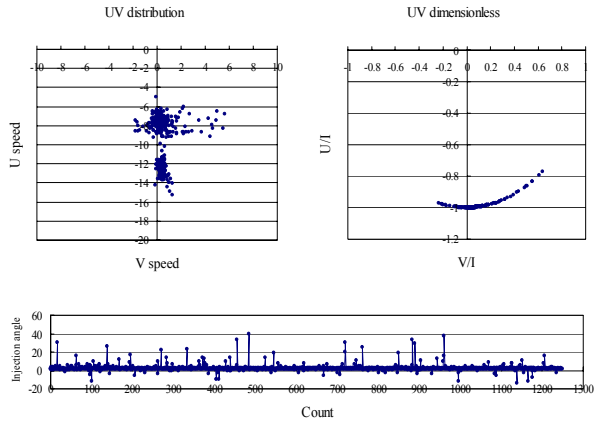

Fig. 15 The injection angle derived from the above data.

For easy reading, the axial velocity is shown in the way downward. On the bottom, the figure shows the histogram of the injection angle.

3.6 Results of Commercial Print Head

For comparison, a commercial print head with black ink was used to generate the referenced data. The reflective mode and the 73 degree location of collection optics from forward scatter in the PDA system were used. The results show that among the data in an injection, more or less the higher axial velocity is, the lager the drop size (see the main and satellite drops shown in Fig. 2). However, the radial velocity is not relative to the drop size. The results also show that the main drop is only about 30% of the measured data.

Closer examination among the data reveals that the drop can be classified into four groups; main drops, medium, smaller and much smaller satellites and their mean diameter are 37 μm, 30 μm, 23 μm and 20 μm, respectively. It is worthy to mention that the smallest mean spray angle (θ_{mean}) is about 0.70° and corresponds to the group of main drops; 2.39° corresponds to the group of medium satellites and 6.85° corresponds to the group of smaller satellites. This fact indicates that the moving path for different group of drop is different. For spray angle, they are 0.78°, 1.44°, 2.82° and 3.72°, respectively, from the main to much smaller drop group. According to Eq. (1), the diameters of circular areas of drop placement are 43.81 μm, 42.57μm, 47.61 μm and 52.47 μm, respectively. Concerning the difference of the moving path, the diameter of circular area of drop placement for the commercial print head will not be smaller than 52.47 μm and the resolution for the ink-jet printing is estimated to be 53 μm.

3.7 Stability of Injection

The stability of injection for different nozzle hole in the same purposed built print head was also investigated by using the water and measuring drop velocities and sizes. The results of different nozzle hole reveal that the mean size ranges from 25 to 36 μm and the smallest and largest standard deviation of the injection angles (σ) are 0.91° and 3.24°, corresponding to the spray angle with 5.46° and 19.44°, respectively. This fact indicates that there is variation in the injection character for different nozzle in the same print head. Therefore, the following measurement

was kept at the same nozzle hole for different fluids.

3.8 Injection Characters of Different Injecting Rates & Fluids

At the same nozzle hole, measurements were carried out for different injecting rates and fluids, respectively. The results reveal that the standard deviation of the injection angle (σ) is affected by the injecting rate; it will be much larger especially in the case with 5 kHz injecting rate.

For size, the mean diameter is not affected much by the injecting rate for the case of water-sugar solution with lower viscosity. But it will be affected for the case of higher viscosity such as the water-sugar solution (33.3%wt) and water-glycerin solution (40%wt); the mean diameter will decrease when the injecting rate reaches 3 kHz and more. This result is consistent with the result of Parrado and González's work [14]; they attributed this fact to the timing being not enough to fill the fluid into the injection chamber.

For comparison, the measured drop velocities (U and V) were divided by I and their standard deviations were listed in the table 2.

Table 2 Standard Deviation of U/I and V/I for Different Fluids

	PF solution (Anisole + TMB) (0.7%wt)	water-glycerin solution (40%wt)	water-sugar solution (25%wt)	water
$\sigma_{U/I}$	0.0009	0.0051	0.0036	0.0143
$\sigma_{V/I}$	0.0149	0.0342	0.0267	0.0585

The results reveal that the variation of the axial velocity component is less than that of radial velocity component, which indicates that the axial velocity component is much more stable than radial velocity component. Closer examination among the values listed on the table 2 reveals that the more viscous is, the more stable of injection. It should be mentioned that it is difficult to inject the PF solution into the ambient. The compromised way is that the nozzle chamber of the print head was filled with water. The pre-injection was carried out first to make sure of emitting and then the PF solution was filled into the chamber to keep continuously emitting.

It is worthy to exam how the fluid property affect the drop size. Figures 16-19 show the velocity-size results for different fluids and indicate that in general, the larger drop carries larger axial velocity.

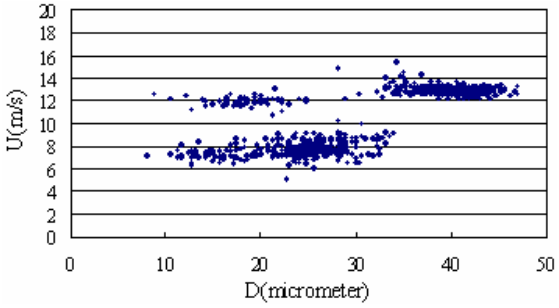

Fig. 16 The velocity-size results for water.

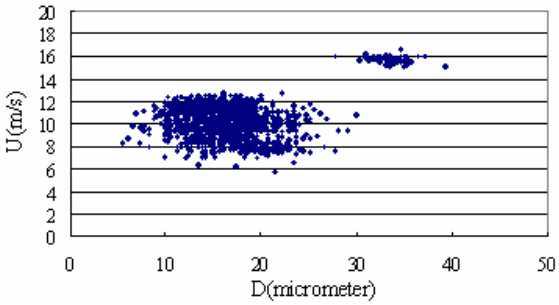

Fig. 17 The velocity-size results for water-sugar solution (25%wt).

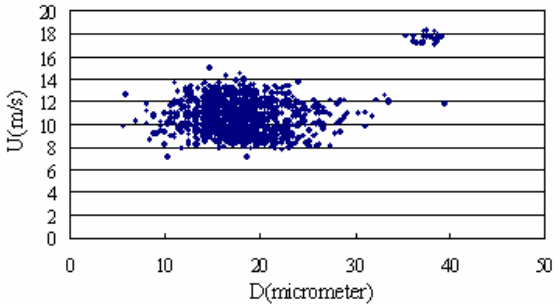

Fig. 18 The velocity-size results for water-glycerin solution (40%wt).

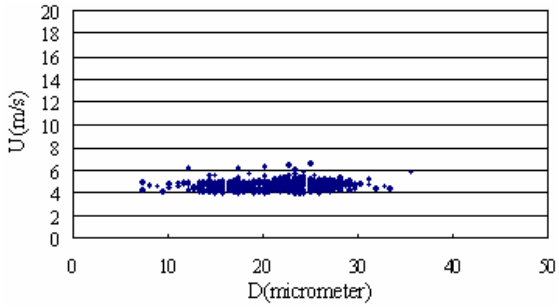

Fig. 19 The velocity-size results for PF solution (Anisole + TMB)(0.7%wt).

Closer examining the result reveals that some small drops carry almost the same velocity with main drop but its velocity will not larger than that of main drop. It is worth mentioning that for all fluids, the acquired number of the larger drop with larger velocity is much smaller than the other drops indicating that the number of main drop is much smaller than that of the satellite. Moreover, the drop diameters are almost ranging from 10 to 30 μm except water and the variation of the axial velocity of PF solution is much smaller. The results also show that increasing the viscosity will decrease the drop size and the decreasing number of larger drop will increase the velocity of smaller drop.

It should be mentioned that the drop after detaching will not shape in spherical in the beginning; therefore it will not be accepted by the PDA measurement if it passes through the measuring volume in a non-spherical shape. The validation rate was examined and table 3 lists the results for acquiring 1,250 samples.

Table 3 Required time for acquiring 1,250 samples and validation rate.

	PF solution (Anisole + TMB) (0.7%wt)	water-glycerin solution (40%wt)	water-sugar solution (25%wt)	water
Required time for acquiring 1,250 samples (ms)	5190.94	471.03	1283.97	1073.05
PDA validation rate(1/ms)	0.24	2.65	0.97	1.16

The results reveal that one firing will produce more than one validated sample for the cases of water and water-glycerin solution which can be attributed to the satellite. For water-sugar solution, the fact that the validation rate is less than 1.0 can be attributed to the longer break up length resulting in more number of non-spherical drops passing through the measuring volume (see figure 5).

As the same way presented in Fig. 15, figure 20-23 show the results of 4 fluids and red lines in the figure indicate the spray angle based on the mean spray angle (θ_{mean}) and the standard deviation of injection angle.

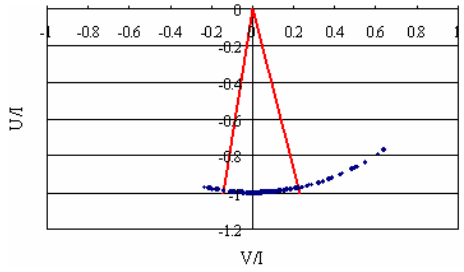

Fig. 20 The dimensionless velocities (U/I, V/I) and spray angle for water.

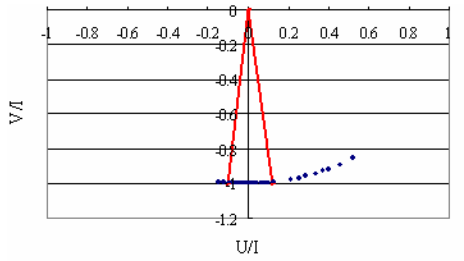

Fig. 21 The dimensionless velocities (U/I, V/I) and spray angle for water-sugar solution (25%wt).

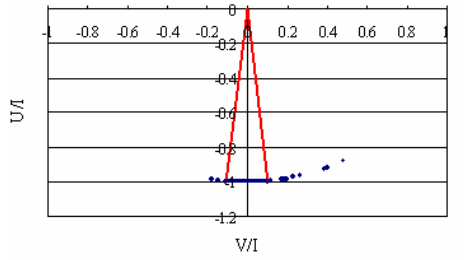

Fig. 22 The dimensionless velocities (U/I, V/I) and spray angle for water-glycerin solution (40%wt).

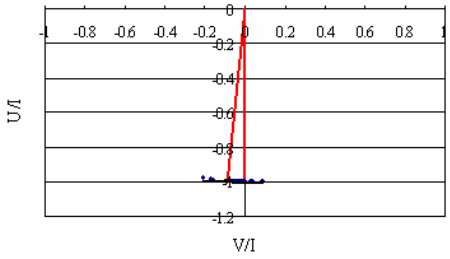

Fig. 23 The dimensionless velocities (U/I, V/I) and spray angle for PF solution (Anisole + TMB)(0.7%wt).

The results reveal that there are some drops flying away from the axis of the nozzle hole and in the same biased direction for all cases. The figures also show that the angular bisectors of the spray angles (mean spray angles) are all close to the axis of nozzle hole, and moreover, in a limit range the more viscous is, the smaller the spray angle. This fact implies that the viscosity of the fluid can reduce the interference of nozzle. For viscosity more than 2.28 cP, this trend becomes opposite except the case of PF solution. These results imply that there are some critical fluid properties resulting in lounger breakup length and smaller spray angle.

Based on the condition of manufacturing, the distance between the substrate and the nozzle exit is about 0.5 mm, therefore the drop placement can be estimated by using Eq. (1) and the results are listed in table 4.

Table 4 The mean diameter, spray angle and diameter of drop placement circular area for different fluids.

	PF solution (Anisole + TMB) 0.7%wt	water-glycerin solution (40%wt)	water-sugar solution (25%wt)	water
Mean diameter (μm)	21.98	18.48	19.04	35.01
Spray angle (degree)	5.12	11.95	9.28	20.87
Diameter of drop placement area (μm)	66.73	123.16	100.19	219.14

The results show that the smallest spray angle will resulting in smallest drop placement area which is about 66μm and reaching the requirement of manufacture's resolution. It should be mentioned again that the longer break up length will result in more satellites. This effect will induce more stable flying since the air drag force will be reduced by the series satellite as mentioned in the work of Parrado and González's [14]. It should be mentioned that the maximum diameter of drop placement circular area excluding the drop size (219.14μm-35.01μm =184.13μm) listed in table 4 is smaller than the length of effective measurement volume (186μm)

4. CONCLUSION

In this paper, the effects of physical properties of at least 4 fluids on the injection character were investigated the feasibility of the manufacturing P-OLED by using the bubble ink-jet printing was assessed. The results of this

study are summarized as follows:
The drop placement accuracy of injection was estimated by alternatively using the spray angle which was derived from the measurements of vertical and horizontal velocities of the droplet. The Particle Dynamic Analyzer (PDA) was used to systematically measure the droplet velocity and size for three fluids in this work. The macro-photography was also used to visualize the detachment process of the liquid jet at the exit of the injector. The typical results are as follow:
1. It is practical to estimate of the drop placement accuracy of injection by deriving from the PDA measured axial and radial velocities and droplet size.
2. In this work, the key factor which controls the accuracy of jet targeting is the breakup length of the injection. The longer breakup length is the more number of satellites. The situation that one satellite follows one closely will induce more stable flying, which results in high accuracy of jet targeting.
3. Under the control of creating acceptable breakup length of injection by selecting suitable physical properties such as the viscosity and surface tension of the working fluid, the manufacturing P-OLED by using the bubble ink-jet printing is feasible.

5. NOMENCLATURE

D	diameter of the circular drop placement [μm]
d_{mean}	mean drop diameter
H	distance between the exit of the nozzle and the measuring point
U	axial velocity (m/s)
V	radial velocity (m/s)
I	length of velocity vector $[(U^2+V^2)^{1/2}]$
α, β	injection angle (degree)
θ_{mean}	mean spray angle (degree)
σ	standard deviation of injection angle (degree)

6. REFERENCES

1. Wu, J. L., Mao, C. Y. and Yang, J. C. Thermal Bubble Micro-fuel Injector, Proc. 13th National Conference on Combustion and Technology, Taiwan, 2003.
2. Leu, T-S. and Lin, Y-H. Fabrication and Diagnostics of A New Ink-Jet Printhead for 3D Rapid Prototyping Applications, Proc. 13th National Conference on Combustion and Technology, Taiwan, 2003.
3. Shiba, S., Yokoi, H., Shirota, K., Sato, H. and Kashiwazaki, A., Color Filter and Method for Manufacturing it, US Patent 5552192, September 3, 1996.
4. Kashiwazaki, A., Nakazawa, K., Hirose, M., Yokoyama, M., Yamashita, Y. and Shirota, K., Color Filter Manufacturing Method, Color Filter Manufactured by the Method, and Liquid Crystal Device Employing the Color Filter, US Patent 6399257, June 4, 2002.
5. Hayes, D. J., Wallace, D. B. and Boldman, M. T. Picoliter Solder Droplet Dispension, ISHM, 1992 Proc., pp. 316-321. 1992.
6. Bale, M., Carter, J. C., Creigton, C., Gregory, H., Lyon, P. H., Ng, P., Webb, L., and Wehrum A., Ink-jet Printing: The Route to Production of Full Color P-OLED Displays, CDT Research Paper, January, 2006.
7. Le, H. P., Progress and Trends in Ink-jet Printing Technology, J. Imaging Sci. and Tec., Vol. 42, pp. 49-62, 1998.
8. Chang, J-C., Tsai, K-C. and Chern, J., Effects of Light-Absorbing Droplets and Optical Factors on a Phase Doppler Particle Size Analyzer, Proc. of ICLASS-'97, August 18-22, 1997.
9. Chang, J-C., Chu, C-S. and Chen C-Y., The Study of Effects of the Refractive Index Changing on a Phase Doppler Particle Analyzer, Proc. of ICLASS-2000, July 16-20, 2000.
10. Chang, J-C., Lu, J-Z. and Yu L-H., Experimental Study of the Effects of Fluid and Wall Surface Properties on Droplet Impingement, Proc. 6th Annual Conference on Liquid Atomization and Spray Systems-Asia (ILASS-Asia '01), pp. 100-105, 2001.
11. Chang, J-C., Huang, S-B. and Lin C-M., Effects of Inlet Surface Roughness, Texture, and Nozzle Material on Cavitation, Atomization and Sprays, vol. 16, pp. 299-317, 2006.
12. Yanta, W. C., Turbulence Measurements with a Laser Doppler Velocimeter, report NOLTR 73-94, Naval Ordinance Labs, White Oak, Silver Spring, 1973.
13. Tate, R. W., Some Problems Associated with the Accurate Representation of Droplet Size Distribution, Proc. of ICLASS-'82, Wisconsin USA 12-4, pp. 341-351, 1982.
14. Parrado, M. E. and González, J. E. Hydrodynamic and Thermodynamic Characterization of In-Flight Droplets Generated by Thermal Ink-jet Print-Heads, Proc. of ICLASS-2000, July 16-20, 2000.
15. Chang, J-C., Shen, M-S. and Lu, J-Z The Effects of Nozzle Geometry and Fluid Property on the Breakup Length of Capillary Jet, the Transactions of the Aeronautical and Astronautical Society of the Republic of China, Vol.32, No.4, pp. 315-321, 2000.

Acknowledgement

This work was supported by the National Science Council, R.O.C. under the contracts NSC 93-2212-E-014-008 and the print head was provided by the Industrial Technology Research Institute .